

# Medical application of diffraction enhanced imaging in mouse liver blood vessels<sup>\*</sup>

ZHANG Xi(张汐)<sup>1,2</sup> YUAN Qing-Xi(袁清习)<sup>3</sup> YANG Xin-Rong(杨欣荣)<sup>4</sup> LI Hai-Qing(李海清)<sup>5</sup>  
CHEN Yu(陈雨)<sup>3</sup> CHEN Shao-Liang(陈绍亮)<sup>1,2;1)</sup> ZHU Pei-Ping(朱佩平)<sup>3</sup> HUANG Wan-Xia(黄万霞)<sup>3</sup>

1 (Department of Radiology, Cancer Hospital, Fudan University, Shanghai 200032, China)

2 (Department of Nuclear Medicine, Zhongshan Hospital, Fudan University, Shanghai 200032, China)

3 (Institute of High Energy Physics, Chinese Academy of Sciences, Beijing 100049, China)

4 (Liver Cancer Institute, Zhongshan Hospital, Fudan University, Shanghai 200032, China)

5 (Cardiovascular Disease Institute, Zhongshan Hospital, Fudan University, Shanghai 200032, China)

**Abstract** Neovascularization is correlative with many processes of diseases, especially for tumor growth, invasion, and metastasis. What is more, these tumor microvessels are totally different from normal vessels in morphology. Therefore, observation of the morphologic distribution of microvessels is one of the key points for many researchers in the field. Using diffraction enhanced imaging (DEI), we observed the microvessels with diameter of about 40  $\mu\text{m}$  in mouse liver. Moreover, the refraction image obtained from DEI shows higher image contrast and exhibits potential use for medical applications.

**Key words** diffraction enhanced imaging, blood vessel, rocking curve, image contrast

**PACS** 42.25.Fx, 87.59.B, 87.61.Jc

## 1 Introduction

Neovascularization is involved in a wide variety of physiological and pathological conditions in our body, including wound repair, metabolic diseases, inflammation, cardiovascular disorders, and tumor progression<sup>[1]</sup>. Especially in the field of tumor research, there is now substantial evidence that tumor growth is angiogenesis-dependent, and that neovascularization is necessary for tumor invasion and metastasis<sup>[2]</sup>. Without neovascularization, the tumor is limited to 2 mm, and cannot be invasion and metastasis. What's more, the tumor microvessels are totally different from normal vessels in morphology. If these microvessels can be demonstrated, the tumor can be found in very early stage and this will be very helpful for medical diagnosis. Therefore, observation of neovascularization has attracted interest of many researchers in the field.

However, conventional radiography cannot provide sufficiently clear images of vessels with a diameter of 200  $\mu\text{m}$  or less and has considerable limita-

tions for imaging microvessel. Therefore, there is a growing interest in using X-ray phase contrast imaging to image blood vessels<sup>[3–6]</sup>. X-ray phase contrast imaging is a recently developed imaging technique, which is approximately 1000 times more sensitive than conventional absorption contrast when imaging the soft tissue<sup>[7, 8]</sup>. Many imaging methods of phase contrast imaging such as X-ray interferometry, diffraction enhanced imaging (DEI) and in-line phase contrast imaging have been developed and used for medical samples. It was reported that blood vessels with a diameter of about 50  $\mu\text{m}$  have been observed without using contrast agent by means of the X-ray interferometry<sup>[3]</sup>, the X-ray optics and the experimental procedure which was very complicated. What's more, the image contrast of 50  $\mu\text{m}$  vessels was not so good.

As one of the phase contrast imaging methods, DEI has been accomplished by inserting an analyzer crystal in the beam path between the sample and the detector. Because DEI can be much more easily implemented, it has become one of the most widely

Received 18 December 2008

<sup>\*</sup> Supported by National Natural Science Foundation of China (30471652)

1) Corresponding author, E-mail: chen.shaoliang@zs-hospital.sh.cn

©2009 Chinese Physical Society and the Institute of High Energy Physics of the Chinese Academy of Sciences and the Institute of Modern Physics of the Chinese Academy of Sciences and IOP Publishing Ltd

used imaging methods since Chapman<sup>[9]</sup> first described it, especially for synchrotron radiation X-ray source<sup>[10–16]</sup>.

In this paper, we studied the mouse liver blood vessels under different DEI imaging conditions and assessed the quality of those images obtained at different positions of the monochromator - analyzer crystal rocking curve.

## 2 Materials and methods

### 2.1 Animals and surgical procedures

Three, 6-week-old female C57BL mice (weighing about 25 g) were anesthetized by an intraperitoneal injection of ketamine (200 mg/kg body weight). Then, the inferior vena cava, superior vena cava and the hepatic pedicle (including the arteries, hepatic veins and common bile ducts) near the porta hepatis were ligated and the livers were excised for imaging. All experiments were conducted in compliance with the guidelines on Animal Care and Use Committee.

### 2.2 DEI experiments

DEI experiments were performed at the 4W1A Topography & Imaging Station of the Beijing Synchrotron Radiation Facility (BSRF). The experimental set-up is schematically shown in Fig. 1. The wiggler source of Beamline 4W1A was 43 m away from the experiment hutch. The X-ray beam incident to the sample has a size of 20 mm (horizontal) × 11 mm (vertical) with the divergence of 0.47 mrad (horizontal) × 0.26 mrad (vertical)<sup>[15]</sup>. The electron beam energy in the storage ring was 2.5 GeV with a current of 150–250 mA. The white X-ray beam from the 4W1A wiggler was monochromatized by a perfect silicon crystal. After passing through the sample, the X-ray was refracted by an analyzer crystal which is the same as the monochromator crystal and detected by a 1300 pixels × 1030 pixels X-ray CCD with the pixel size of approximately 10.9 μm × 10.9 μm (X-ray Fast Digital Imager 18 mm camera system, Photonic-Science Ltd., UK). Al filters with different thicknesses were used to attenuate the X-ray of low energy. The DEI experiments were first carried out by using Si (111) diffraction plane and then using Si (333) diffraction plane of the same two crystals with 15 keV X-ray. Samples were mounted on a scanning stage driven by stepping motors and images were acquired when the analyzer crystal was set at different positions of the rocking curve of the analyzer/monochromator system.

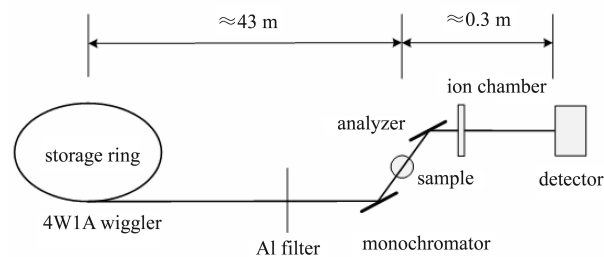


Fig. 1. Schematic DEI experimental set-up at 4W1A Beamline of BSRF.

### 2.3 Image evaluation

The minimum diameter of visualized blood vessels was measured using Image J1.37v Preferences Program (National Institutes of Health, USA), which identified both of the blood vessel edges by expressing a density curve in combination with a 256 gray-scale image. Two of the periphery vessels were chosen in each quarter of the image and the diameter of each vessel was measured by two authors respectively. The minimum vessel diameter, as determined by two separate measurements, was averaged and used to express the minimum vessel diameter in each image.

In order to quantitatively compare the contrast of images obtained at different positions of the rocking curve, the following equation was used to roughly calculate the contrast in the groups<sup>[16]</sup>.

$$C = \frac{I_1 - I_2}{I_1 + I_2}, \quad (1)$$

where,  $I_1$  and  $I_2$  were the gray values on either side of the blood vessel wall as measured with Image J1.37v Preferences Program. Four periphery areas (smallest vessels) were chosen in each image to calculate the contrast respectively. The four calculated contrasts were averaged and used to express the contrast of the smallest vessels in each image.

## 3 Experimental results

From Fig. 2, we can see that the images obtained using Si (333) diffraction plane are clearer than those obtained using Si (111) diffraction plane and have higher image contrast. The effects of edge enhancement and three-dimensional appearance of images acquired using Si (333) diffraction plane are significantly superior to the images obtained using Si (111) diffraction plane. Images obtained at FWHM positions (Figs. 2(a), (c), (d), (f)) show the enhanced and highlighted edges of features as if a shadow is cast on a three-dimensional surface. This shadowing effect is reversed between the images of different sides of rocking curve: the bright edge in image Figs. 2(a) and (d) appears dark in image Figs. 2(c) and (f).

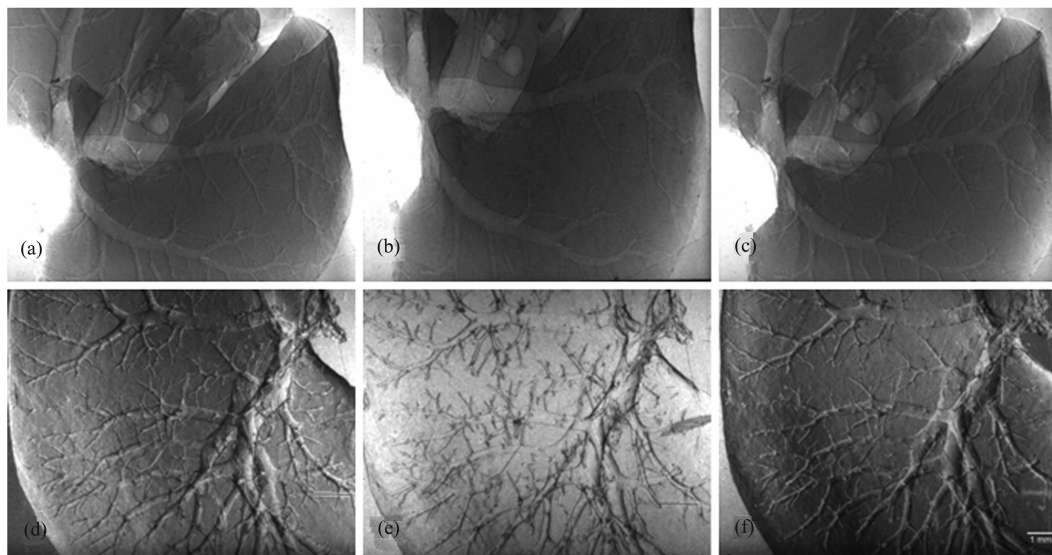


Fig. 2. The DEI images with larger field of view. (a)—(c) are acquired using the Si (111) diffraction plane; (d)—(f) are acquired using the Si (333) diffraction plane; (b) and (e) are taken when the analyzer crystal is set at the peak position of the rocking curve; (a) and (d) are taken when the analyzer crystal is tuned to one side of FWHM position of the rocking curve; (c) and (f) are taken when the analyzer is tuned to the other side of FWHM position of the rocking curve.

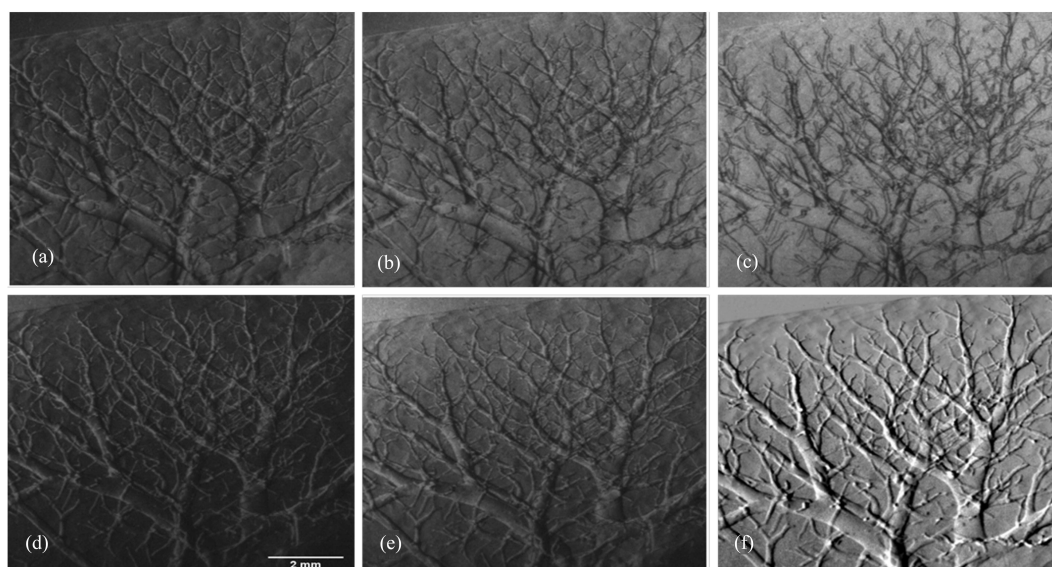


Fig. 3. Detailed appearances of blood vessels in local area of mouse liver. Image (a) and (d) were acquired at both tails, (b) and (e) at both FWHM and (c) at the peak of the rocking curve; Image (f) is the refraction image.

Compared with the peak images (Figs. 2(b) and (e)), the images taken at the FWHM positions of the rocking curve (Figs. 2(a), (c), (d) and (f)) have greater contrast and better image quality. Moreover, the edges of vessels and the correlation of vessels were also demonstrated clearly by those FWHM images.

As can be seen from Figs. 2(d), (e) and (f), we could observe the vessels branching pattern to the eighth generation of branch. The eighth generation of branches still has a high contrast against the liver tissue. The vessel diameter decreased according to each

generation of branching and as a function of the distance from the main axial vein toward the periphery. According to the measurement using Image J1.37v Preferences Program, the diameter of the smallest vessels was approximately  $40\ \mu\text{m}$ .

Figs. 3(a)—(e) show the images taken at different positions of the rocking curve. The positions are schematically shown as Fig. 4. Images in Figs. 3(a) and (d) acquired at both tails show greater edge enhancement and strong three-dimensional appearance, but the image noise also is increased greatly. There-

fore, the images are difficult to interpret. The images in Figs. 3(b) and (e) recorded with the analyzer set to the FWHM position of the rocking curve, where the variation in reflectivity with angle is of opposite slope, show high image contrast and opposite shadowing effect.

Fig. 3(f) is the refraction image obtained by subtracting two raw images in Figs. 3(b) and (e) pixel by pixel<sup>[9, 17]</sup>. The refraction image seems to have the highest image quality than the images obtained at different positions of the rocking curve, moreover, the refraction image has high sensitivity for delineating the boundaries of those regions in the object that have different refractive indices.

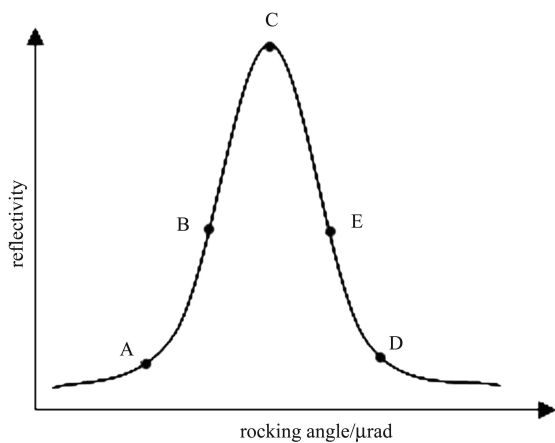


Fig. 4. Schematic obtaining positions of rocking curve for Fig. 3 images (a)–(e).

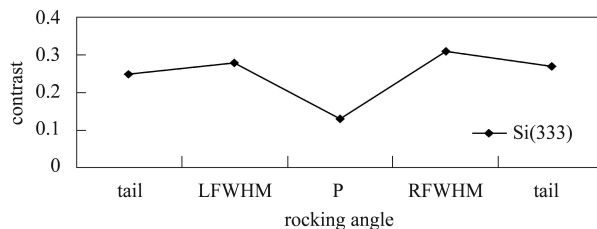


Fig. 5. Contrast of the smallest vessels in Figs. 3(a)–(e) plotted with respect to the analyzer crystal positions.

At different positions of the rocking curve, the contrast of the smallest vessels in those images seems different. Using Eq. (1), the contrast of the smallest vessels in Figs. 3(a)–(e) is calculated as Fig. 5. From Fig. 5, we can see that the images taken at the FWHM position show the highest contrast. The contrast of the smallest vessels in refraction image (Fig. (f)) was also calculated using Eq. (1), with the result of 0.55, which is higher than that of the FWHM images. Thus, the refraction image is the most applicable DEI image for imaging blood vessels.

## 4 Discussion

Imaging neovascularization is critical for early diagnosis and treatment of tumors and infarcted diseases. Currently, many new therapeutic approaches have been opened for us to some life-threatening diseases by controlling angiogenesis in the affected organs. In cancer therapy, for example, modulation of factors responsible for tumor angiogenesis may be beneficial in inhibiting tumor progression<sup>[1]</sup>. Moreover, in many circulatory disorders, there is substantial involvement of small vessels and obtaining a clear picture is crucial for an accurate prognosis and proper treatment strategy. Therefore, if we can demonstrate these deformed microvessels, the tumor and some diseases have a great chance to be radically cured in very early stage.

From the formally published references, the smallest blood vessel that has been detected is about 30  $\mu\text{m}$  in diameter, under the condition of using a physiological saline as contrast agent<sup>[4, 18]</sup>. Without contrast agent, the smallest blood vessel that has been detected is about 50  $\mu\text{m}$  in diameter<sup>[3]</sup>. All those two results were obtained using the X-ray interferometry method and do not have good microvessel contrast. The biggest disadvantage of the X-ray interferometry is the need of complicated X-ray optics and experimental procedure, as a consequence, this imaging method cannot be easily performed as one wants.

Our experimental results show that the blood vessels of about 40  $\mu\text{m}$  in diameter can be demonstrated clearly without using contrast agent. What's more, the imaging method we used is DEI, the set-up of which is very simple and can be performed easily. In addition, when the analyzer crystal was positioned on different angular settings, different sensitivities on tissues and their interfaces were provided. It was reported that the DEI peak images exhibited a distinct improvement in the contrast of calcifications when compared with the images obtained at other positions of the rocking curve<sup>[10]</sup>. However, to the best of our knowledge, it is still not very clear at what's position of the rocking curve the best imaging quality of blood vessels can be obtained. According to our experimental results, the images obtained at the FWHM positions of the rocking curve were superior to the peak image, and that the refraction image obtained by subtracting two FWHM images showed the highest image quality.

For refraction image, the effects of the refraction are “doubled” by subtraction of the two opposite

slope images pixel by pixel. The subtraction also suppresses the featureless background<sup>[17, 19]</sup>. Therefore, refraction image is very useful in highlighting boundaries or edges in heterogeneous regions within the object. Although the refraction images depict strong edge enhancement, this is not gained at the expense of increased image noise, as would generally be the case when spatial filtering is used to sharpen images. This opens new opportunities for imaging based on these properties. Thus, the refraction image is the most applicable DEI image for medical diagnosis.

In DEI experiment, when imaging on the shoulder of the rocking curve, the change of refraction angle  $\Delta\theta$ , which is caused by micro-structures of the sample, will produce corresponding change of X-ray intensity  $\Delta I$ , resulting in the enhanced contrast. For X-rays with the same energy, the FWHM of Si (333) rocking curve is several times narrower than that of Si (111), i.e., the rocking curve of Si (333) crystals is sharper than that of Si (111), therefore, for the same

sample, which means the same  $\Delta\theta$ , it will produce several times bigger  $\Delta I$  in Si (333) set-up than in Si (111) set-up, resulting in higher image contrasts. This is the key reason that the blood vessels of about 40  $\mu\text{m}$  in diameter can be demonstrated clearly by using the Si (333) diffraction plane.

## 5 Summary

DEI can provide a larger field of view and higher image quality but it does not need complicated X-ray optics and experimental procedure. Using the DEI method, fine vessel details down to the 40  $\mu\text{m}$  scale can be revealed clearly. Especially, the refraction image obtained from DEI provides a good delineation of the boundaries of the blood vessels and exhibits potential use for medical applications.

*The work was done at the 4W1A Topography & Imaging Station of the Beijing Synchrotron Radiation Facility (BSRF).*

## References

- 1 Furuya M, Nishiyama M, Kasuya Y et al. *Vascular Health & Risk Management*, 2005, **1**(4): 277—290
- 2 Pluda J M, Parkinson D R. *Cancer*, 1996, **78**(3 suppl): 680—687
- 3 Momose A, Takeda T, Itai Y. *Radiology*, 2000, **217**: 593—596
- 4 Takeda T, Momose A, WU J et al. *Circulation*, 2002, **105**: 1708—1712
- 5 Momose A, Takeda T, Itai Y. *Acad. Radiol.*, 1995, **2**: 883—887
- 6 Hwu Y, Tsai W L, Je J H et al. *Phys. Med. Biol.*, 2004, **49**: 501—508
- 7 GAO D, Pogany A, Stevenson A W et al. 1998, **18**: 1257—1267
- 8 Momose A, Takeda T, Itai Y et al. *Nat. Med.*, 1996, **2**: 473—475
- 9 Chapman D, Thomlinson W, Johnston R E et al. *Phys. Med. Biol.*, 1997, **42**: 2015—2025
- 10 Kiss M Z, Sayers D E, ZHONG Z et al. *Phys. Med. Biol.*, 2004, **49**: 3427—3439
- 11 LIU Chen-Lin, YAN Xiao-Hui, ZHANG Xin-Yi et al. *Phys. Med. Biol.*, 2007, **52**: 419—427
- 12 Mollenhauer J, Aurich M E, ZHONG Z et al. *Osteoarthritis Cartilage*, 2002, **10**: 163—171
- 13 LI J, ZHONG Z, Lidtke R et al. *J. Anat.*, 2003, **202**: 463—470
- 14 JIANG Xiao-Ming, LI Gang, CHEN Zhi-Hua et al. *HEP&NP*, 2004, **28**: 1282 (in Chinese)
- 15 YUAN Qing-Xi, TIAN Yu-Lian, ZHU Pei-Ping et al. *Nuclear Techniques*, 2004, **27**: 725—728 (in Chinese)
- 16 Pagot E, Fiedler S, Cloetens P et al. *Phys. Med. Biol.*, 2005, **50**: 709—724
- 17 ZHANG Xi, LIU Xiao-Song, YANG Xin-Rong et al. *Phys. Med. Biol.*, 2008, **53**: 5732—5743
- 18 LIU Chen-Lin, YAN Xiao-Hui, ZHANG Xin-Yi et al. *Nuclear Techniques*, 2006, **29**: 885—890 (in Chinese)
- 19 ZHU Pei-Ping, YUAN Qing-Xi, HUANG Wan-Xia et al. *Acta. Phys. Sin.*, 2006, **55**: 1089—1090 (in Chinese)